Power Dissipation Studies and Damping of Power Fluctuations in The Presence of an IntegratedPower Dissipation Controller Using a New Algorithm

Hossein Nasir Aghdam , Mehdi Mohammadi
Department of Electrical Engineering. Ahar Branch, Islamic Azad University, Ahar, Iran
h_nasir59@yahoo.com,mehdi_mohammadi_power@yahoo.com

Abstract

The most important goal of power system operators is to provide the power required by the consumer at a constant voltage, without harmonics and with a certain frequency. The optimal situation in the production and transmission system is that this system should be able to produce the desired power and the desired consumer. This demand is usually considered in the initial design, but over time due to changes such as: consumption growth, connection of other networks to the previous network, construction of new lines and power plants, etc., upset this balance and put some restrictions. They create power in the operation of the network. In the early days of power systems, they were relatively simple and were designed to be able to operate independently. In addition, transmission system designers have found that AC transmission systems must be controlled by devices to respond to dynamic conditions. Transmission systems were first controlled by classical power control devices under constant conditions or slow load changes and current power control and voltage changes. The dynamics of the system were performed with large stability ranges to cover the critical conditions predicted by faults, line and generator outages, and equipment faults. These factors made transmission systems less efficient and the only solution needed to power them was to build new lines. Therefore, the use of FACTS and D-FACTS devices was proposed, which solved many of the above problems and has a higher efficiency.

1. Introduction :

Stopping electromechanical oscillations is one of the main concepts related to the performance of the electrical power system. If these oscillations are not properly controlled, they may lead to partial or total system shutdown. The main reason for the maintenance and growth of fluctuations is the lack of a proper damping system. The distribution of electrical power through an alternating transmission line is a function of the line impedance, the magnitude of the transmitter and receiver voltages, and the phase angle between them. Compared to the mechanical key control of the transmission system, the power electronics comply with the FACTS devices are faster and have more flexibility. The advantage of semiconductor technology speed is the superiority of using switching power converters in power systems. Different types of FACTS devices are used for dynamic control of voltage, impedance and phase angle of high voltage AC transmission lines, which makes it possible to operate a transmission line up to close to the thermal capacity. Changing the impedance of transmission lines and then controlling the power dissipation allows damping and filtering of unwanted transients on the transmission system. Flexible AC Transmission System (FACTS) is used today in power systems to improve both the steady state and the dynamic performance of systems. The UPFC Integrated Power Distribution Controller is the most sophisticated, pervasive, interesting, and possibly most expensive and highly adaptable FACTS member that uses synchronous voltage sources (SVS) to control power dissipation, introduced by Gayogi in 1991.

The initial UPFC model has been tested in the United States and South Korea. In this research, the issue of power distribution control and quenching power fluctuations in the presence of an integrated power distribution controller (UPFC) in the power network is investigated. These two fundamental challenges are posed as an optimization problem. For this purpose, the work is done on two levels. At the first level, it is a question of extracting the fixed value of UPFC, controller and network, which will be optimally obtained using a new and powerful group search optimization algorithm (GSO). In the second level, the effect of UPFC presence on damping power fluctuations and power distribution, by installing UPFC on a power system, will be studied. With this explanation, the case study will be performed in two levels. In the first level, the optimization problem is solved by coding in mfile environment to extract fixed number values and then by installing UPFC on a power grid, power fluctuation curves And power distribution will be obtained in Simulink environment.

2. Analysis and Modeling

Due to the complex nature of UPFC and the need to study and analyze its effects on the power grid, various techniques for analyzing and modeling UPFC have been published in the past literature. Reference [1] proposes a new method for compensating reactive power in microgrids with DFIG based on air-diesel system in order to achieve voltage stability of the combined system with the presence of UPFC. For this purpose, small single model wind-diesel system, DFIG based on wind turbine system, UPFC and controllers have been designed for stability analysis. In addition, voltage change and reactive power compensation have been analyzed using UFFC-based ANFIS. Simulation in MATLAB environment is performed for transient stability analysis in a micro-grid-based wind-diesel system with different wind power input and 20% increase in load. The simulation results show the efficiency and superiority of the proposed method and affect the transient behavior of the microgrid. In [2], an analysis and study of the characteristics of subsynchronous resonance (SSR) of the compensation system coupled with the Generalized Integrated Power Distribution Controller (GUPFC) has been performed. Various modes of operation of series and parallel converters have been proposed to investigate the effect of SSR characteristics. SSR analysis methods with GUPFC are designed based on damping torque evaluation, system eigenvalues and transient simulation. The damping torque is calculated by considering the D-Q model for GUPFC to determine the torsional stability.

3. Control System Design

One of the main challenges in using FACTS devices is how to control it and in fact the design of the controller. How it is controlled has a direct impact on UPFC responses. Therefore, in [3-4], various techniques for controlling UPFC have been proposed. Martinez et al. [18] proposed a separate active and reactive sliding mode control for the UPFC. The third harmonic output voltage controller for a full bridge converter is able to extract active power from the third harmonic current in order to maintain the DC voltage limits of the

converter. Sliding mode controllers (DPFCs) simultaneously inject active and reactive power at the base frequency for independent control of active and reactive power distribution. Another feature of the proposed controller is the possibility of applying a controlled sliding mode to a part of the orange distribution network and the transmission network under study. In [5], radial basis function (RBFNN) neural network controllers for UPFC are designed to improve the transient stability performance of the power system. RBFNN uses both a single nerve or a neural structure and dynamically regulated parameters. The performance of the neural controller designed using single-trigger and three-machine systems for various transient disorders is evaluated. In the case of a three-machine 8-bus power system, the performance of a single-neural RBF controller is compared with a back-diffusion (BF) algorithm based on a multilayer neural network controller. The new RBFNN controller for UPFC provides better damping performance compared to existing PI controllers. Operation and use in the network Reference [6] provides a differential relaying program for the transmission line in the presence of UPFC and wind farm. The process begins with the recovery of the fault current signal in the respective busbars connected to the fault lines and reprocessing using wavelet transform to generate approximate third level coefficients (CA3). Discrete Fourier transform (DFT) is then used to calculate the effective value of the signal generated by the reconstructed signals in terms of approximate turret coefficients. By estimating the RMS value of the signal, the exploited and reconstructed values are calculated for error elimination and classification in transmission lines with UPFC and wind farm. The proposed design is carefully tested in error conditions with extensive changes in operating parameters and the test results show the ability to detect and classify errors. Reference authors [7] have used genetic algorithms (GA) and differential evolution (DE) to minimize line losses and simultaneously reduce operating costs of three types of FACTS devices, which are: TCSC, SVC and UPFC. Optimal placement of FACTS devices in the power system reduces line losses, controls reactive power dissipation, improves node voltage profiles and reduces operating costs. The proposed technique is tested on the IEEE 30-bus system for optimal adjustment of FACTS devices. Finally, the performance of the system using UPFC compared to FACTS series and parallel devices is compared.

4. Application of UPFC for Different Purposes

A. Oscillation damping: Adaptive particle cluster optimization based on nonlinear time-varying acceleration coefficients (NTVAC-PSO) has been proposed to solve the oscillation optimization and damping problems in the presence of UPFC in [8]. The new method helps to control the overall search ability of the original PSO algorithm and increase its convergence rate with a reasonable response in less repetition. A set of well-known optimization problems has been tested to prove the strength of the proposed algorithm and the results have been compared with other similar techniques. In [9], GA technique is used for simultaneous stability of power systems using UPFC.

GA is used to find the optimal location of UPFC and its control parameters are set in different operating conditions. The problem is formulated using a multi-objective optimization problem that helps optimize the damping rate of electromechanical states. This method has been successfully tested on the 69-bus 16-machine system in the New York-New England integrated system and on the Iraqi National Power System to quench the local and internal states of fluctuations. In addition, the proposed method demonstrates the superiority of performance compared to fuzzy-based UPFC controller.

B) Improving dynamic behavior:

In [10], the dynamic model of the power system is presented with a new UPFC that includes two shunt converters and a series capacitor. In this structure, a series capacitor is installed between two shunt converters to inject the desired series voltage. As a result, it is possible to control the distribution of active and reactive power. The main merit of the proposed UPFC Compared to its conventional structure is the injection of series voltage waveform with a total harmonic distortion (THD). In addition, a linear Philip-Hefron model is obtained and a complementary controller is proposed for the proposed UPFC modeling. The new controller-based UPFC problem is formulated as a time-based objective function optimization problem solved using PSO techniques and the Colonial Competition Algorithm (ICA). Reference [11] has proposed a new method for optimal UPFC positioning (OUPFC) as a controller of power distribution under random conditions by satisfying practical decisions. Random analysis has been performed to detect and rank fault probabilities based on review of electrical power systems. Medium load minimization on all power transmission lines is considered as the optimal objective function, while network settings are also implemented to minimize active power losses. This optimization problem is optimized using nonlinear programming structure (NLP) and using CONOPT solver.

C) Power distribution:

Reference [12] proposes an alternative to steady-state modeling of UPFC by setting current constraints. The proposed flow model assumes that the current behaves as a variable in the optimal power dissipation problem. The performance of the proposed model and the power injection model are compared through the Gauss-Newton optimization method. Two operating conditions in the 39 medium voltage bus network have been studied from the point of view of optimization and current limitations. In [13], the power dissipation control amplitudes of a simple system are evaluated and compared by obtaining an injectable compensated series voltage injection by the transformer and UPFC. The transformer response time is usually long and depends on the pulse rate. In evaluating power distribution control ranges and voltage stability ranges, the transmission line of the system is modeled in four different ways. The results of different line models are also compared. In [14], the control of the supports in the electrical power system is performed using UPFC. Attributed models for combining power distribution programs have been evaluated and analyzed. The application of UPFC to control the optimal power dissipation through numerical results is

shown. These results show that a UPFC has the ability to regulate power dissipation and minimize power losses simultaneously. The performance of UPFC is compared with Schiff phase transformer (PST).

5. UPFC Construction

The main components of UPFC are two voltage source inverters (VSIs) with a strong DC capacitor and connected to the power system via a coupling transformer. [15] The shunt inverter or STATCOM is connected to the system via a shunt transformer. Which injects a controlled sinusoidal current with a variable size at the junction. STATCOM compensates for reactive power at the transmission line while keeping the DC voltage constant at the same time during the DC connection [16]. The series inverter is activated if the DC terminal (positive or negative) of the line is required to maintain a constant Vdc capacitor voltage. Therefore, the net active power absorbed from the line by UPFC is only equal to the losses of their inverters and transformers. The remaining capacity of the shunt inverter can be used as the reactive power exchanged with the line to regulate the voltage at the connection point [15]. The reactive power of the shunt converter can be independently controlled and modeled as a controllable reactive power source. Therefore, to obtain the general model, the reactive power injected into the bus i must be added to the series branch model (3). The general model is shown in Figure 4 [17]. Two inverters can be considered as sources, so UPFC devices include two three-phase back-to-back [17] self-conducting [17] GTO converters and a DC connection formed by a strong DC capacitor [18]] (See Figure (2-9)). The two voltages are synchronous with each other, but with a difference in magnitude due to the reduced voltage of the shunt transformer [19]. The energy storage capacity of a dc capacitor is usually small, so the active power drawn by the shunt converter must be equal to the active power generated by the series converter [20]. The UPFC injects AC series into the voltage transmission line and regulates the power distribution by controlling the amplitude and phase of the voltage [17]. Converter 1 is coupled by a shunt transformer (excitation transformer) and converter 2 is coupled by a series transformer (step-up transformer) [1]. The shunt converter is able to change the active and reactive powers according to the system, which can compensate the shunt independently [17]. With two converters, UPFC can not only provide reactive power but also active power. The equations of active and reactive power are [19]:

$$P_{12} = \frac{V_s V_r}{X_{sr}} \sin \delta \quad (1)$$

$$Q_{12} = \frac{V_s V_r}{X_{sr}} (\cos \delta + 1) \quad (2)$$

The power distribution capacity of the AC system is controlled by adjusting the injection voltage. The line current and the injector voltage determine the series of mixed injection power required by the converter. The active injection power of the series converter must be obtained from the DC connection, which itself is supplied from the AC system through the shunt converter. When excluding losses of converters and coupling transformers, the UPFC active power balance relationship is [21].

$$P_{se} + P_{sh} = 0 \quad (3)$$

UPFC can theoretically be located anywhere along the line. From a practical point of view, the factors influencing site selection include cost, availability, fault level, protective relay specifications, and impact on improving power system performance. If the UPFC system is located in the middle of the line, it is very suitable in terms of accessibility, monitoring, security. If the line is at the end.

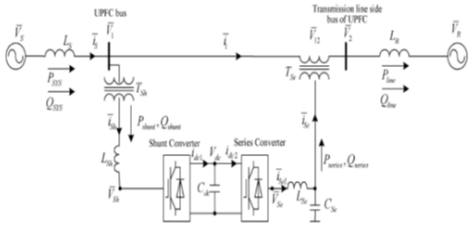

Fig.1. UPFC building

6. - The UPFC Model Used in the Simulation

Figure (2) shows the general model of the UPFC connected to the power grid. To design a power flow control system and oscillation damping, UPFC must first be modeled in the network. In this dissertation, the flow injection model is used to model the UPFC. As shown in Figure (3), the UPFC modeling uses a dependent voltage source instead of a series converter and a dependent current source instead of a shunt converter.

7777777777

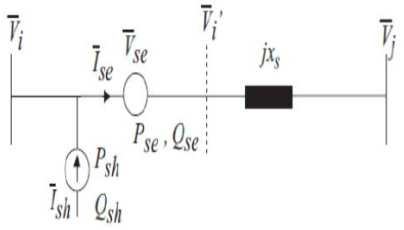

Fig.2. Equivalent circuit of UPFC converters in the studied transmission system453333

In the above figure, the shunt converter current (Ish) can be decomposed into the following two-phase components with voltage Vi (It) and perpendicular to it (Iq) as follows.

$$\tilde{I}_{shunt} = \tilde{I}_t + \tilde{I}_q \qquad (4)$$

Vse are the ideal voltage conversion instead of jxs1 series converters and transmission line reactance. Vse series voltage sources are amplitude and phase control variables. We also have:

$$\tilde{V}_{s1} = M_B \tilde{V}_i e^{j\delta_E} \qquad (5)$$

By converting Vs1 voltage sources to Iinj current sources, UPFC current injection is obtained. This model is shown in Figure (3).

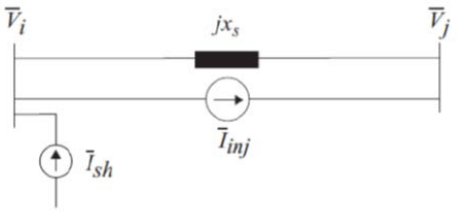

Fig.3. UPFC flow injection model

According to Figure (3) we have:

$$\bar{I}_{INJ} = \frac{\bar{V}_s}{jx_s} = -jb_{s1}m_b\bar{V}_i e^{j\delta_E} \qquad (6)$$

In the above equation, bs1 = 1 / xs1 are the transmission line suspensions and mb and δE are the amplitude and phase of the injected voltages relative to the voltage. Hence, it can be written:

$$P_{CONV1} = \mathrm{Re}\left[\bar{V}_i\left(-\bar{I}_{sh}\right)\right] = -V_i I_i \qquad (7)$$

$$S_{s1} = \bar{V}_{s1}\bar{I}_{ij}^{*} = M_B\bar{V}_i e^{j\delta_E}\left[\frac{\bar{V}_i - \bar{V}_j}{j(x_{s1})}\right]^{*} \qquad (8)$$

$$S_{s1} = P_{s1} + jQ_{s1} \quad (9)$$

Given the above relationships we have:

$$\begin{cases} P_{s1} = (b_{s1})\left(M_B V_i V_j \sin(\theta_i - \theta_j + \delta_E) - M_B V_i^2 \sin(\delta_E)\right) \\ Q_{s1} = (b_{s1})\left(M_B V_i V_j \cos(\delta_E) - 2M_B V_i^2 - M_B V_i V_j \cos(\theta_i - \theta_j + \delta_E)\right) \end{cases} \quad (10)$$

The active power absorbed by the converter in parallel with the power system is calculated from Equation (11):

$$P_{shunt} = \mathrm{Re}\left[\bar{V}_i \left(-\bar{I}^*_{shunt}\right)\right] = -V_i I_i \quad (11)$$

From the above equations,

$$\begin{cases} -V_i I_t = (b_{s1})\left(M_B V_i V_j \sin(\theta_i - \theta_j + \delta_E) - M_B V_i^2 \sin(\delta_E)\right) \\ \bar{I}_{shunt} = \bar{I}_t + \bar{I}_q = (b_{s1})\left(-M_B V_j \sin(\theta_i - \theta_j + \delta_E) + M_B V_i \sin(\delta_E)\right) \end{cases} \quad (12)$$

Therefore, the parameters of the UPFC flow injection model are obtained from the following equations according to Figure (3).

$$\bar{I}_{Si} = \bar{I}_{shunt} - \bar{I}_{s1} \quad (13)$$

$$\bar{I}'_{sj} = \bar{I}'_{s2} \quad (14)$$

Finally we can write,

(15)

$$\bar{I}_{Si} = (b_{s1})\left(-M_B V_j \sin(\theta_i - \theta_j + \delta_E) + M_B V_i \sin(\delta_E)\right) + b_{s2} M_B \bar{V}_i e^{\delta_E} \quad (16)$$

$$\bar{I}'_{Sj2} = -jb_{s2} M_B \bar{V}_i e^{\delta_E}$$

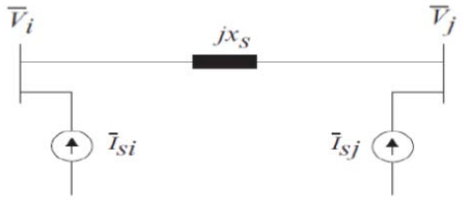

Fig.4. Modified UPFC flow injection model

7. Group Search Optimizer

The population The GSO algorithm is called a group and each person in the population is a member. In a n-dimensional search space, the i-th member in the repeated k-th search has the current position X¬ik∈Rn and the vertex angle Φik = (Φi1k,…, Φki (n-1)) ∈Rn-1. The search path of the i member, whose unit vector is Dik (Φik) = (di1k,…, dki (n-1)) ∈Rn, can be calculated using a polar for Cartesian synchronous conversion.

$$d_{i_1}^k = \prod_{q=1} \cos\left(\phi_{i_q}^k\right) \quad (17)$$

$$d_{i_1}^k = \sin\left(\phi_{i_{(j-1)}}^k\right).\prod_{q=1} \cos\left(\phi_{i_q}^k\right) \quad (j = 2, ..., n-1) \quad (18)$$

$$d_{i_1}^k = \sin\left(\phi_{i_{(j-1)}}^k\right) \quad (19)$$

For example, in a 2D search space, if in the k-iteration the value of the vertex angle is equal to Φik = (π / 3, π / 4), using the relation (11) of the unit vector of the search path is equal to Y = (1/2, √6 / 4, √2 / 2) Dik is obtained.

In GSO, a group consists of three types of members: generator and searcher and scattered members. In order to converge the calculation, it will be tried that there is only one generator in each search iteration and the rest are considered as search members. Dispersed limbs also move randomly. In the simplest integration policy, it is assumed that all search engines use the resources found by the generator.

7 – 1 - Productive :

In the k iteration, the generator status is specified using the vector Xpk = (xkp1,…, xkpn). This vector scans the three surrounding points for a better position.

First, the generator scans the position of the point in front,

$$X_F = X_P^k + r_1 l_{\max} D_p^k \left(\phi^k\right) \quad (20)$$

Second, the generator scans the point on its right,

$$X_F = X_P^k + r_1 l_{\max} D_p^k \left(\phi^k + r_2\,\theta_{\max}/2\right) \quad (21)$$

Third, it scans the point on its left,

$$X_F = X_P^k + r_1 l_{\max} D_p^k \left(\phi^k - r_2\,\theta_{\max}/2\right) \quad (22)$$

Where r1 is a random number with a normal distribution of mean and standard deviation of 1. r2 is a random number with normal distribution in [0,1]. θmax maximum tracking angle and lmax maximum tracking distance:

$$l_{\max} = \|U - L\| = \sqrt{\sum_{j=1}^{n} \left(U_j - L_j\right)^2} \quad (23)$$

Where Uj and Lj are the top and bottom edges of the search space, respectively.
If the generator of the best position is three points better than the current position, it moves to the best position and its angle changes as a relation (24):

$$\phi^{k+1} = \phi^k + r_2 \alpha_{\max} \quad (24)$$

Where αmax is the maximum tracking angle. Otherwise it will remain in its original state. If the generator fails to find a better position in iteration a, it scans the opposite side as relation (25):

$$\phi^{k+a} = \phi^k \quad (25)$$

7 – 2 - Checker :

In the calculation, many members are selected as searchers. If the i member is selected as a checker in the k iteration, it moves to the generator at a random distance:

$$X_i^{k+1} = X_i^k + r_3.\left(X_p^k - X_i^k\right) \quad (26)$$

Where r3 is a uniform random distribution in the interval [0,1].

7 – 3 - Ranger :

The remaining members of the group are called Rangers. If the i member is selected as a ranger in the k iteration, it is converted to a random angle as a relation (25) and calculates the search path using relations (17) to (19). Moves towards random effluent in the following relation:

$$l_i = a.r_1 l_{\max} \quad (27)$$

$$X_i^{k+1} = X_i^k + l_i.D_i^k\left(\varphi^{k+1}\right) \quad (28)$$

8. - Execution of GSO Algorithm

Set k = 0

Random initialization Xi and vertex angle φi of all members Calculation of fitness values of primary members: f (Xi)

As long as (stop conditions are not met)

For (each member i in the group)

Select a generator: Find the Xp group generator **Production implementation:**

The generator scans at a zero angle and then samples from three points in the scan range using Equations (17) to (19)

• Find the best with the best source (amount of fit) . If the best point has a better source than the current situation, it moves to that point . Otherwise, it remains in its current state and determines its path using Equation (25) .

• If the generator is not able to find a better area after iterations a, it converts its angle of motion to zero using (26).

Search : Randomly select 80% of the remaining members

To search Dispersal For the remaining members, they will disperse from their current status for sorting:

• Generating a random motion angle using equation (25)

• Select a random distance l¬I using Equation (27) and move to a new point using (28).

Fit Calculation: Calculate the fit of an existing member f (Xi)

Complete while setting k = k + 1 Implementation

9 - Implementation of GSO algorithm on the problem:

At the end of the third chapter, how to optimize the problem is discussed. The main challenge is to calculate and determine the UPFC control parameters to extract the most optimal value possible . For this purpose, simulation is performed at two levels. First code with m file and then extract the output from simultic.

Step 1. Target the problem

The main purpose of the research is to extract the optimal values for the UPFC control parameters. In such a way that by damping the velocity, the lowest possible values are produced for Kp (derivative interest rate) and Ki (integral interest rate).

Step 2 . objective function

Define the objective function The objective function of the problem is defined as follows:

$$OF = T_s .SimOut_{ac} + T_s .SimOut_{re} \quad (29)$$

Where, Ts : runtime

SimOutac: The absolute value of active power feedback SimOutac : The absolute value of reactive power feedback

Step 3. Execute the algorithm :

At this point, the optimization starts by specifying four variables for the GSO algorithm. The reason for choosing the four variables is the existence of Kp and Ki for both active and reactive powers . By targeting Equation (29), the optimal values for Kp and K¬i are calculated.

Step 4. Linking :

So far, the GSO algorithm has been able to generate optimal values for the objective function. In order to be able to use these optimal values in the simulation process in Simulink environment, the control parameters of the PI controller were not numbered and written as Kp and Ki, so that the values of these parameters can be extracted and quantified based on the optimal values.

Step 5. Extract the results

By running Simulink, the curves related to the studied parameters are extracted.

9 - simulation :

In the simulation process, the GSO algorithm is used to adjust and extract the values of the fixed number parameters. The desired curves are extracted with the programming link done in mfile environment to Simulink. Figure below shows how the UPFC is placed in the network. It is assumed that the UPFC is installed between the two busbars B1 and B2. Bus B1 is connected to the power supply and bus B2 is connected to the power grid. The general specifications of the equipment in the power network are reviewed below. In this section, the simulation results of the simulation are presented. For this purpose, the results are first presented for the optimized parameters and how the problem

converges. In the second and third sections, the resulting curves of dynamic behavior and power distribution will be presented.

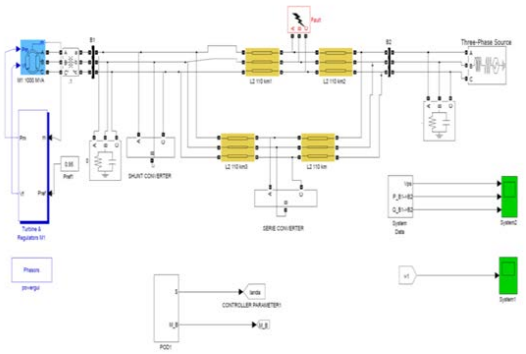

9 – 1 - The objective function :

In the first part of the presentation of the results, we study the objective function and convergence for 20 times of program execution. In Figures (5) to (9), Kp and Ki, respectively, are presented for the active and reactive powers, and finally the objective function.

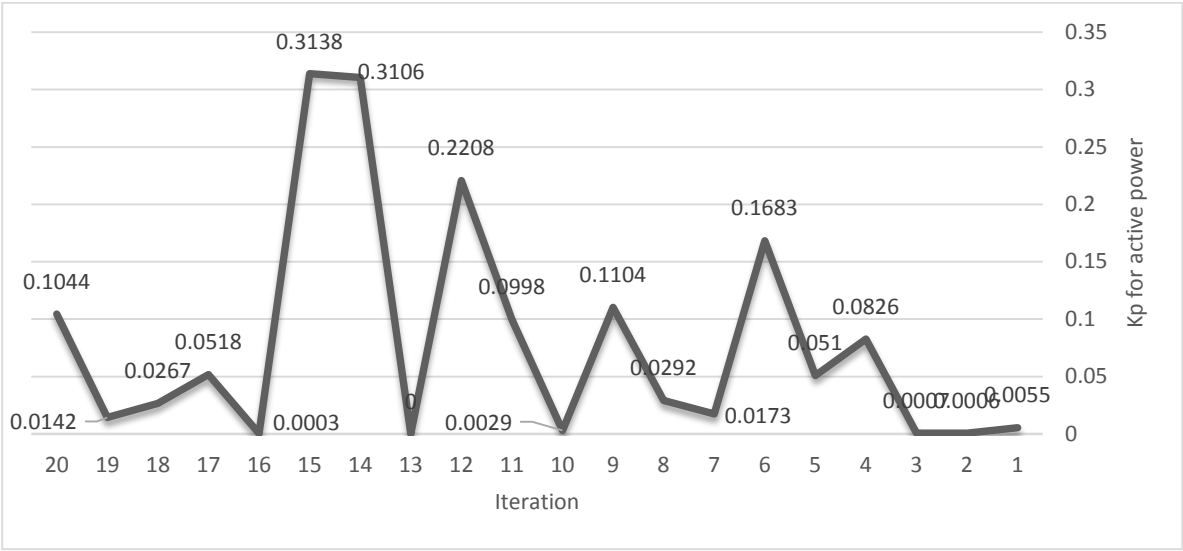

Fig.5. The resulting responses for the Kp active power parameter

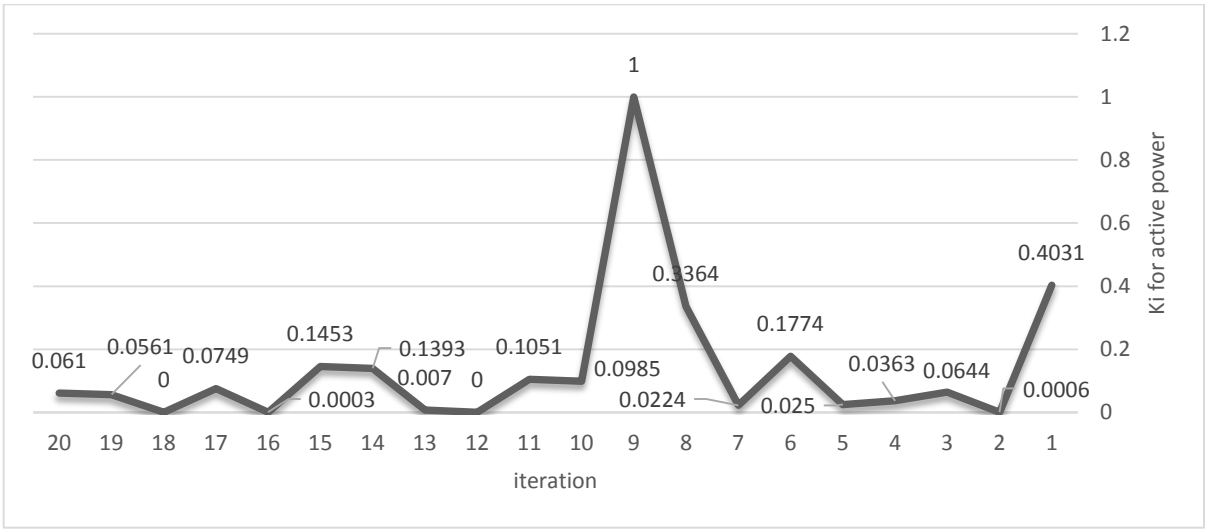

Fig.6. The resulting responses for the active power Ki parameter

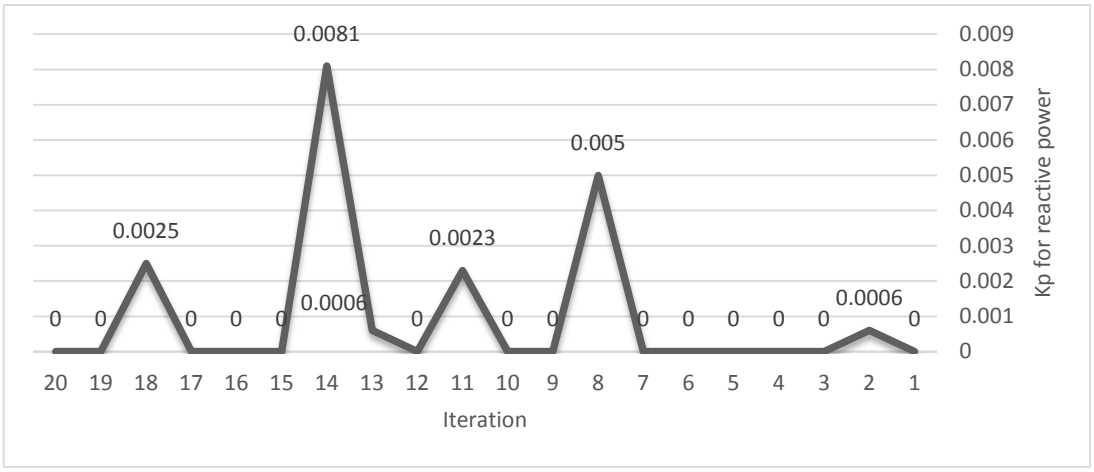

Fig.7. The resulting responses for the Kp parameter of reactive power

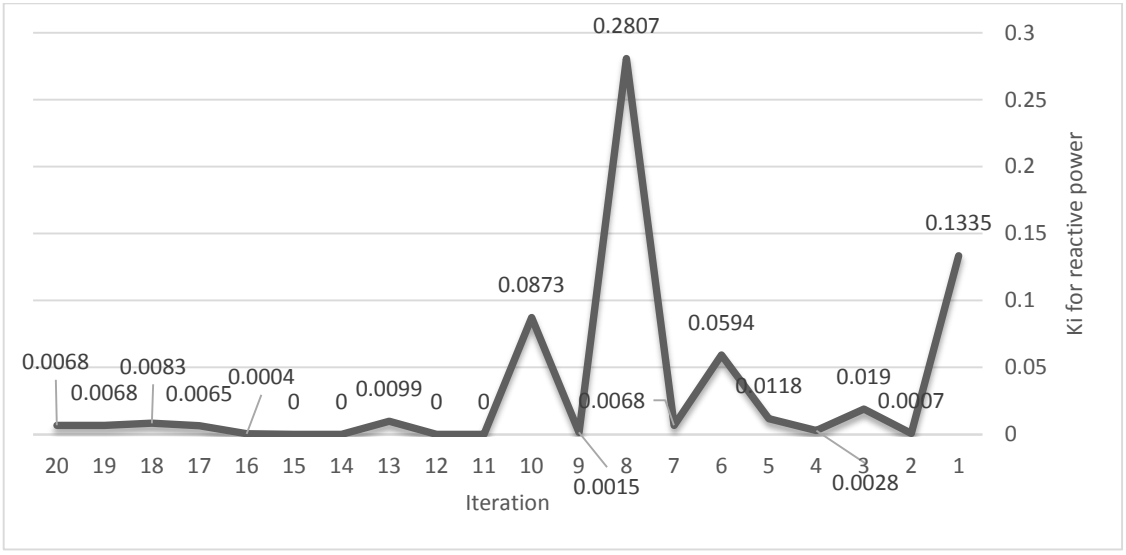

Fig.8.The resulting responses to the reactive power Ki parameter

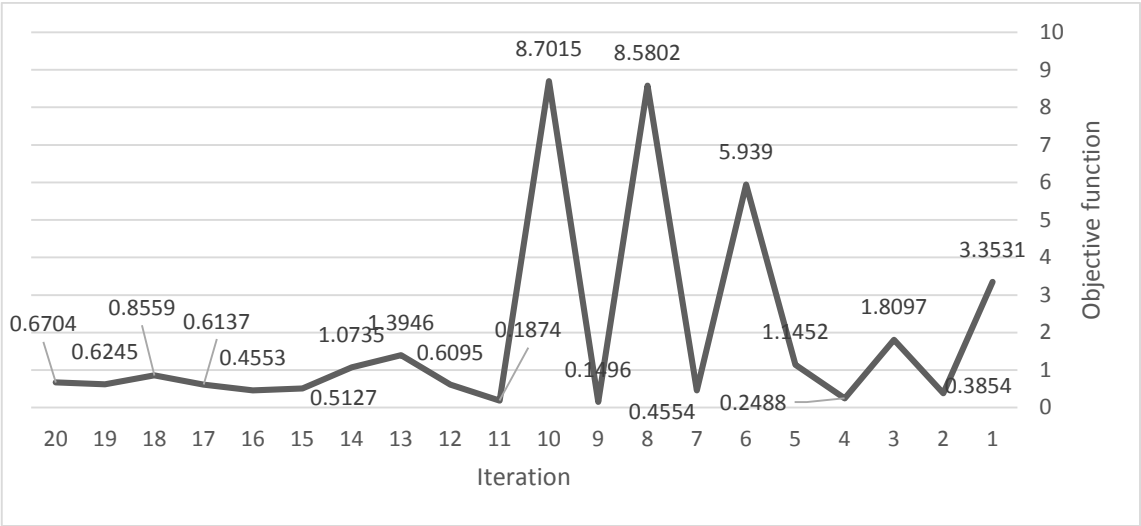

Fig.9. The resulting answers to the objective function parameter of the problem

From Figure (9) it can be seen that the best possible answer to the problem is obtained in the ninth iteration . How the problem converges in the best possible answer can be seen in Figure (10).

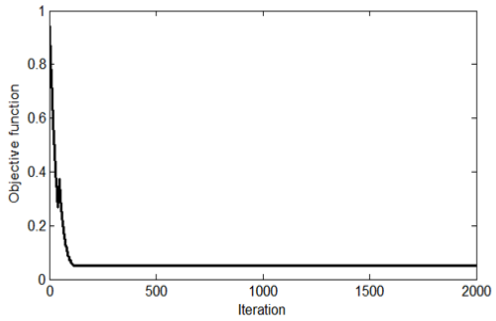

Fig.10. How the problem converges

9 – 2 - Dynamic behavior :

Figure (11) shows the dynamic responses per velocity. Carefully in this figure, we can say that the miraging was done in the first cycle. In other words, except for the first cycle, in other cycles, damping is done properly. The upper and lower boundaries do not exceed 1.025 and 0.96, respectively.

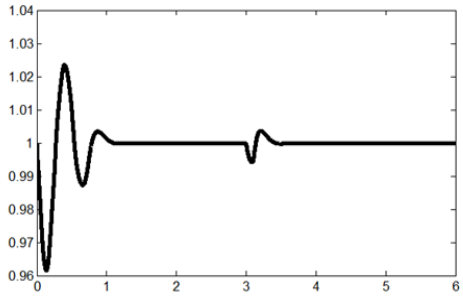

Fig.11. Dynamic responses for velocity

Figure (12) shows the converted power between the two busbars B1 and B2 between which the UPFC is installed. To be precise in this figure, it can be claimed that although the distortion occurred in the middle cycles, it returned to the same 5000 in the rest of the curve. At the start, that number has risen to more than 16,000.

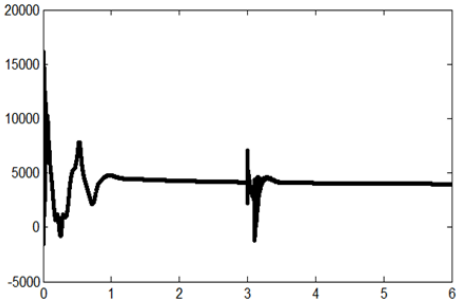

Fig.12. Converted power between two busbars

Changes in the Landa control parameter can be seen in Figure (13). It can be said that this curve has a behavioral pattern similar to Figure (12). The maximum and minimum range of changes are 9 and 6-, respectively.

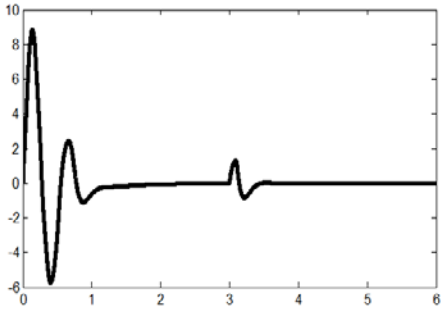

Fig.13.Changes in Landa control parameter in dynamic behavior

Finally, in Figure (14), the amount of bus voltages B1 and B2 can be seen.

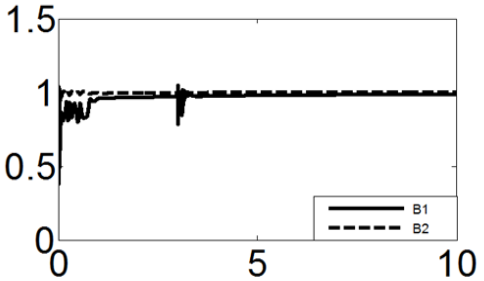

Fig.14. The values of bus voltages B1 and B2

9 – 3 - Power distribution:

In the third part of the results, the effect of the study on the parameters affecting the power distribution is presented. Figure (15) shows how the active power of the network changes. According to Figure (15), it can be said that the change in active power in 10 seconds is such that its quasi-sinusoidal behavior can be observed, except for a few relatively large distortions. The amount of change is from 500 to 1000 and after the initial cycle, it has started to change from close to 1000. Figure (16) shows the reactive mode of this power.

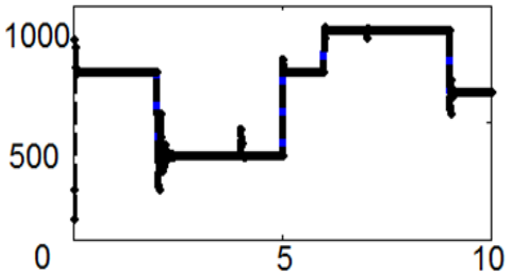

Fig.15. Changes in the active power of the network

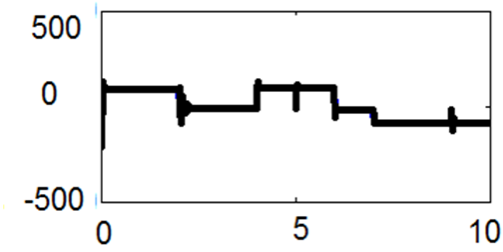

Fig.16. Changes in the reactive power of the network

Based on what is shown in Figure (16), the range of reactive power changes is less than Aknio power and the pattern of sinusoidal changes is not observed. At about the fifth second, the highest level of reactive power can be seen. Figure (17) shows the Landa signal changes in the power dissipation study.

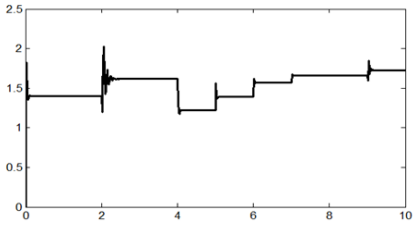

Fig.17. Changes in Landa control parameter in power distribution

According to Figure (17), the range of change is between 1- and 2. At each moment of the value change, a significant distortion occurs, with the greatest possible distortion occurring in the second. Convergence similar to the state of dynamic behavior is not observed.

Conclusion

In this dissertation, the problem of dynamic behavior of the power grid is improved by installing UPFC in it. In formulating the problem, one of the main challenges of power networks is to reduce the fluctuations and improve the dynamic behavior of the network. The problem is optimized using the GSO algorithm. The GSO algorithm is one of the newest group optimization algorithms that has not been used seriously in solving power system problems. In the process of extracting the results, four basic parameters have been considered, which are: dynamic responses per velocity, converted power between two busbars, control parameter changes, and bus voltage values B1 and B2. From the simulation results shown in Figures 8 to 10, it can be argued that distortion usually occurs in the middle cycles. The first cycle has the worst possible response and the most severe distortions. The two converted power curves between the busbars and the dynamic responses for velocity have a similar pattern of behavior.

Reference

[1] Mohanty A., Viswavandya M., Ray K.R., and Patra S., Stability analysis and reactive power compensation issue in a microgrid with a DFIG based WECS, International Journal of Electrical Power & Energy Systems, 2014, 62, 753-762.

[2] VyakaranamB., and VillasecaF.E., Dynamic modeling and analysis of generalized unified power flow controller, Electric Power Systems Research, 2014, 106, 1-11.

[3] MartinsI.M., SilvaF.A., PintoS.F., and MartinsI.E., Sliding mode active and reactive power decoupled control for distributed power flow controllers, Electric Power Systems Research, 2014, 112, 65–73.

[4] P. K. Dash, S. Mishra, and G. Panda, A radial basis function neural network controller for UPFC, IEEE Transactions on Power Systems, 2000, 15(4), 1293-1299.

[5] Malhotra U., and Gokaraju R., An Add-on self-tuning control system for a UPFC application, IEEE Transactions on Industrial Electronics, 2014, 61(5), 2378-2388.

[6] TripathyL.N., JenaM.K., and SamantarayS.R., Differential relaying scheme for tapped transmission line connecting UPFC and wind farm, International Journal of Electrical Power & Energy Systems**,** 2014, 60, 245-257

[7] BhattacharyyaB., GuptaV.K., and KumarS., UPFC with series and shunt FACTS controllers for the economic operation of a power system, Ain Shams Engineering Journal [in press]

[8] EslamiM.,ShareefH., Raihan TahaM., and M. Khajehzadeh, Adaptive particle swarm optimization for simultaneous design of UPFC damping controllers, International Journal of Electrical Power & Energy Systems, 2014, 57, 116-128.

[9] HassanL.H., MoghavvemiM., AlmuribH.A.F. , and SteinmayerO., Application of genetic algorithm in optimization of unified power flow controller parameters and its location in the power system network, International Journal of Electrical Power & Energy Systems, 2013, 46, 89-97.

[10] BanaeiM.R., Seyed-ShenavaS.J., and FarahbakhshP., Dynamic stability enhancement of power system based on a typical unified power flow controllers using imperialist competitive algorithm, Ain Shams Engineering Journal, 2014, [in press]

[11] Lashkar AraA., AghaeiJ., Alaleh M., and BaratiH., Contingency-based optimal placement of Optimal Unified Power Flow Controller (OUPFC) in electrical energy transmission systems, Scientia Iranica, 2013, 20(3), 778-785.

[12] Pereira M., and Cera Zanetta L., A current based model for load flow studies with UPFC, IEEE Transactions on Power Systems, 2013, 28(2), 677-682.

[13] Haque M.H., Power flow control and voltage stability limit: regulating transformer versus UPFC, IEE Proc.-Gener. Transm. Distrib., 2004, 151(3), 299-304.

[14] Noroozian M., Angquist L., Ghandhari M., Anderson G., Use of UPFC for optimal power flow control, IEEE Transactions on Power Delivery, 1997, 12(4), 1629-1634.

[15] Tara Kalyani S., and Tulasiram Das G., Simulation of real and reactive power flow control with upfc connected to a transmission line, Journal of Theoretical and Applied Information Technology, 2008, 16-22.

[16] Mailah N.F., Bashi S.M., Marium N., and Aris I., Simulation of a three-Phase multilevel unified power flow controller UPFC, Journal of Applied Scientific, 8(3), 2008, 503-509.

[17] Noroozian M., Angquist L., Ghandhari M., Anderson G., use of UPFC for optimal power flow control, IEEE Transactions on Power Delivery, 12(4), 1997, 1629- 1634.

[18] Mete Vural A., and Tumay M., Mathematical modeling and analysis of a unified power flow controller: a comparison of two approaches in power flow studies and effects of UPFC location, Electrical Power and Energy Systems, 29, 2007, 617-629.

[19] KennedyJ., and R.EberhartR., Particle swarm optimization,Proceedings of IEEE International Conference on Neural Networks IV, 1995, 1942-1948.

[20] BaykasoluA., zbakır L. and TapkanP., Artificial bee colony algorithm and its application to generalized assignment problem, Swarm Intelligence, Focus on Ant

and Particle Swarm Optimization, 2007, 113-144..

[21] Dorigo, M., Di Caro G., Ant colony optimization: A new meta-heuristic,Proceedings of the 1999 Congress on Evolutionary Computation (CEC'99), 1999, 1470-1477.

[22] Omid Bozorg Haddad, Abbas Afshar, And Miguel A. Marino, Honey-bees mating optimization (HBMO) algorithm: a new heuristic approach for water resources optimization, Water Resources Management, 2006, 20, 661-680.

[23] Yan X., Yang W., and Shi H., A group search optimization based on improved small world and its application on neural network training in ammonia synthesis, Neurocomputing,2012, 97, 94-107.

[24] Farrag M.E.A., and Putrus Gh.A., Design of an adaptive neurofuzzy inference control system for the unified power-flow controller, IEEE Transactions on Power Delivery, 2012, 27(1), 53-61.

[25] Monteiro J., Fernando Silva J., Pinto S.F., and Palma J., Linear and sliding mode control design for matrix converter based unified power flow controllers, IEEE Transactions on Power Electronics, 2013, 29(7), 3357-3367.